Hadean, Archean, and modern Earth: Zircon-modeled melts illuminate the formation of Earth's earliest felsic crust

T.L. Carley[1], E. A. Bell[2], C.F. Miller[3], L.L. Claiborne[3], T.M. Harrison[2]

[1]Department of Earth and Environmental Geosciences, Lafayette College, 116 Van Wickle Hall Easton, PA 18042, USA

[2]Department of Earth, Planetary, and Space Sciences, UCLA, 595 Charles Young Drive East, Los Angeles, CA 90095, USA

[3]Department of Earth and Environmental Sciences, Vanderbilt University, PMB 351805, 2301 Vanderbilt Place, Nashville, TN 37235-1805, USA

ABSTRACT

The magmato-tectonic environment(s) of origin for Earth's earliest crust are enigmatic and fiercely debated. Revealing the composition of the melts from which Hadean (>4.02 Ga) zircons crystallized might clarify conditions of initial crust construction. We calculate model melts using Ti-calibrated zircon/melt partition coefficients ($Kd_{Zrc(Ti)}$) and published trace element data for Hadean and Archean zircons. The same treatment is applied to zircons from possible analogue environments (MORB, Iceland, arcs, lunar), to constrain potential petrogenetic similarities and distinctions between the early and modern world. Model melts from oceanic environments (MORB, oceanic arc, Iceland) have higher heavy rare earth element (HREE) contents and shallower middle REE (MREE) to HREE/chondrite (ch) slopes than those from continental arcs and tonalite-trondhjemite-granodiorite suites (TTGs). Hadean and Archean model melts are nearly indistinguishable from one another, both resembling TTGs and continental arcs, with pronounced depletion of HREE and slope reversal in heaviest REE. A limited number of samples ≥ 4.25 Ga yield model melts with broadly similar characteristics to those from younger Hadean and Archean zircons, but with relatively elevated REE (~half order of magnitude) and higher LREE and MREE relative to HREE. Rare earth element patterns of early Earth model melts suggest a common petrogenetic history in the Hadean and Archean, involving garnet ± amphibole in relatively low-temperature, high-pressure, environments.

INTRODUCTION

Zircon crystals are the only recognized physical record from the Hadean eon (>4.02 Ga; Harrison, 2020; cf. O'Neil et al., 2008). As relics of silicic magmas, they provide evidence of earliest crustal compositions and crust-constructing processes: U-Pb ages and Ti concentrations reveal timing and temperatures of crystallization (Ferry and Watson, 2007); other trace elements hold clues regarding source materials, tectonic settings, and extent of evolution (Claiborne et al., 2006; Grimes et al., 2007); Hf and O isotopes illuminate mantle and crustal source contributions (Kinny and Maas, 2003; Valley, 2003); and mineral inclusions further document crystallization conditions (Bell et al., 2015; Bell et al., 2017).

Despite the diverse and ever-increasing varieties of evidence that can be extracted from zircon, the petrogenesis of Hadean magmas remains controversial. Some researchers have inferred crystallization in mafic, oceanic, environments (e.g., Kemp et al., 2010; Gréaux et al., 2018); some argue for involvement of subduction (Hopkins et al., 2008; Turner et al., 2020); while others call upon extraterrestrial impacts (Kenny et al., 2016). The debate continues because Hadean zircon crystals are out of context. The magmas in which they crystallized, and thus critical evidence of their petrogenetic histories, are lost to the geologic record.

Knowing the composition of the melts from which Hadean zircons crystallized will permit meaningful comparisons with modern Earth systems, clarifying their magmo-tectonic environment(s) of origin. Partition coefficients (Kds) provide a mechanism for constraining the composition of a melt from which a mineral crystallizes. However, reliable and consistent zircon/melt Kds are elusive. This is because of challenges in determining compositions of zircon and coexisting melts in experimental and natural materials, and because of a wide range of true Kds (Claiborne et al., 2018). Based on measurements of zircon rims and host glasses, Claiborne et al. (2018) demonstrated a strong negative correlation between Kds and zircon saturation temperature for elements including U, Th, and the REE. The Ti concentration in zircon rims is also negatively correlated with Kds, consistent with a temperature dependence of zircon Ti concentration ((Ferry and Watson, 2007). Based on this correlation between temperature and Kds, they calculated equations for Ti-adjusted zircon-melt Kds ($Kd_{Zrc(Ti)}$). These $Kd_{Zrc(Ti)}$, which account for much of the complexity in zircon/melt partitioning behavior, permit unique insight into magmatic systems of the early Earth.

APPROACH

Model melts are calculated using $Kd_{Zrc(Ti)}$ (Claiborne et al., 2018) and published trace element data for Hadean and Archean zircons. The same treatment is applied to zircons from potential analogues (e.g., MORB, Iceland, arcs, hotspots, the Moon). We exclude model values for La, Ce, Pr, and Eu because Claiborne et al. (2018) consider Kds for these elements to be unreliable. Because of their extreme incompatibility, concentrations of LREE (except Ce) are near detection limits and subject to strong influence by inclusions. Oxygen fugacity, a variable not assessed by Claiborne et al. (2018), strongly affects Kds for polyvalent Ce and Eu .

Model melt compositions are compared to one another, and to measured tonalite-trondhjemite-granodiorite (TTG) rock compositions (Moyen, 2011), to identify compositional evidence of petrogenetic similarity (or difference) between the early and modern Earth. We also compare model melts across the Hadean-Archean boundary, in an attempt to temporally constrain a petrogenetic transition into the modern (post-Hadean) world.

Early Earth Zircon Compositions

Early Earth zircon compositions used in this investigation are from compilations in Bell et al. (2016 and 2017) and Carley et al. (2014). Appendix 1 contains supporting references. The Bell et al. (2016 and 2017) compilation contains paired Ti and trace element (TE) compositions, carefully vetted for signs of post-crystallization alteration, for 75 Hadean (4.0 to 4.245 Ga) and 114 Archean (< 4.0 Ga to 3.3 Ga) zircon analyses. These data are primarily from Jack Hills, Australia (177 of 189; Bell et al., 2016); the other 12 are Archean zircons from the Nuvvuagittuq Supracrustal Belt, Quebec, Canada (Bell et al., 2017). To represent the earliest years of Earth's history (≥ 4.25 Ga), the Bell et al. (2016 and 2017) compilation is supplemented by the Carley et al. (2014) compilation (n = 64). These ≥ 4.25 Ga zircons (n = 61 for U; n = 12 for REE) lack paired TE-Ti analyses, so a representative concentration of 5 ppm Ti is used to calculate model melts. This is the median Ti value for both the Carley et al. (2014; n = 600) and Bell et al. (2016 and 2017; n = 76) Hadean compilations. Model melts calculated using this representative concentration are indicated in Appendix 1. Model melt sensitivity to Ti concentration (and thus, the consequences selecting a non-representative Ti value) is depicted in Appendix 2.

Compositions of Zircons from Modern Earth and Lunar Settings

Model melts are calculated using published compositions of zircons from an assortment of well-constrained tectono-magmatic environments: the Moon (Crow et al., 2017) as an analog for magma ocean and/or stagnant lid + plume scenarios; MORB (Grimes et al., 2007); Iceland (Carley et al., 2014); ocean arc (Izu-Bonin: Barth et al., 2017); "evolving rifts" with oceanic lithosphere replacing continental lithosphere (Salton Sea, USA: Schmitt and Vazquez, 2006; Schmitt et al., 2013; Alid, Eritrea: Lowenstern et al., 1997; Lowenstern et al., 2006); and continental arcs (Mount St. Helens, USA: Claiborne, 2011) Yanacocha, Peru: Dilles et al., 2015). Early Earth model melt compositions are also compared to a global compilation of Archean TTGs (Moyen, 2011).

RESULTS

Model melt values are available in Appendix 1, accompanied by original zircon compositions and $Kd_{Zrc(Ti)}$.

We plot model melt and TTG whole-rock compositions using combinations of trace elements commonly used to discern zircon provenance (e.g., Grimes et al., 2007). Hadean and Archean model melts define the high U/Yb – low Y end of a negatively trending compositional spectrum (Fig. 1a). These early Earth values plot near model melts from continental arcs (Yanacocha, Mount St. Helens) and measured TTGs. Conversely, model melts for the Moon, MORB, oceanic arc, Iceland, and evolving rifts have distinctly lower U/Yb and higher Y. Other trace element discrimination schemes (e.g., Yb vs. Y, Th/Yb vs. U/Yb) reveal consistent groupings (Appendix 2).

Chondrite-normalized REE plots (Fig. 2a) display similar compositional distinctions. Again, the early Earth (modeled melts and measured TTG) define one compositional extreme (MREE/ch 7-10, HREE/ch 4-7) and the moon defines the other (all REE/ch > 100). The two continental arc examples are similar to early Earth: Yanacocha is almost identical, while Mount St. Helens has somewhat higher MREE/ch and HREE/ch (20-10). MORB, Iceland, oceanic arc, and evolving rifts have flat to negatively-sloping MREE/ch and HREE/ch (100-20).

The early Earth samples (modeled Hadean and Archean, measured TTG) share an abrupt, hook-like inflection, from decreasing MREE to increasing heavy REE (HREE), with a minimum at Er-Tm. Yanacocha is similar, with a minimum at Ho. Mount St. Helens also falls to a minimum at Ho, but from Ho to Lu its pattern is flat at HREE/ch ~10. The early Earth and continental arc patterns are distinct from model melts representing modern oceanic environments. The oceanic arc plots with a shallow concave-up pattern, with an inflection around Dy, straddling REE/ch ~30; the MORB pattern is flatter with higher REE/ch (~70). The lunar model melt displays an irregular, pronounced, concave-up shape with an abrupt change in slope at Gd. The irregularity is perhaps due to extremely elevated Ti (median Ti = 99 ppm; Crow et al., 2017), far above the values used in the Claiborne et al. (2018) calibration, impacting the integrity of the model.

DISCUSSION

Hadean vs. Archean Model Melts

Model melt compositions calculated using Hadean (≥ 4.0 Ga) and Archean (< 4.0 Ga) zircon populations are almost identical in trace element discrimination (Fig. 1) and REE patterns (Fig. 2). They closely resemble whole-rock TTG compositions (Moyen, 2011). The similarity between Archean model melts and TTG is expected, as >3 Ga felsic rocks are dominantly TTG (Moyen and Martin, 2012). The compositional coherence between the Hadean and Archean is noteworthy, suggesting a common petrogenetic history.

Early Earth Variability through Time

To investigate if model-melts record a transition from the Hadean into an Archean-like world, we compare early Earth model melts divided into 0.25 Ga age bins (4.5-3.0 Ga). The close similarity between Hadean and Archean model melts persists from 4.25 to 3 Ga. Median U/Yb and Y (Fig. 1b), REE/ch (Fig. 2b), MREE/HREE(ch) and Lu/Tm (Fig. 3) are indistinguishable across the Hadean-Archean age boundary. However, the oldest model melts (≥ 4.25 Ga, n = 12 of 192) are consistently distinct from the rest of the early Earth, with lower median U/Yb (1.4 vs. 3.4 to 5.9) and higher median Y (20 ppm vs. 7 to 11 ppm; Fig. 1b). They also have higher median REE abundance by a factor of ~2 to 8 (Fig. 2b). Chondrite-normalized MREE/HREE ratios are elevated for the ≥ 4.25 Ga model melts (e.g. median Sm/Lu ~6.8 vs 3.0 to 4.2; Fig. 3a). The slope reversal in the REE/ch diagram, expressed by Tm/Lu, is greatest in the oldest Hadean model melts (0.94 vs 0.75 to 0.80; Fig. 3b).

While these compositional distinctions are tantalizing, confidence is tempered by the limited number of REE analyses for zircons ≥ 4.25 Ga (n = 12). The lack of Ti for these zircons, requiring application of an assumed value (5 ppm), is also concerning. If Ti was as low as 1-2 ppm, the melt compositions would be closer to the rest of those modeled for the early Earth. However, we consider 5 ppm to be a conservative estimate (typical of Hadean zircon, well below typical values for modern Earth); higher Ti would lead to a greater compositional difference between these oldest model melts and the rest of the early Earth (Fig. 2, Appendix 2). Despite (or because of) these uncertainties, the apparent variation through the Hadean warrants further study, especially of more zircon ≥ 4.25 Ga.

Early Earth Model Melts: Comparison with Melts from Known Settings

Early Earth model melts are consistently distinct from those generated in modern oceanic settings (e.g., MORB, Iceland, ocean arc), evolving rifts, and the Moon. It is therefore unlikely that early Earth zircons crystallized from a magma ocean (cf. the Moon), magmas that formed by shallow melting in environments with elevated geothermal gradients (Iceland, MORB), or more generally from juvenile, mantle-derived, magmas (including ocean arcs).

In contrast, early Earth model melts (and TTG) are very similar to model melts from continental arcs (Mount St. Helens and especially Yanacocha). These model melts are "adakite-like" in their steep, negatively-sloping REE patterns, low to very low HREE, and inflections near Er-Tm (Kay, 1978); they especially resemble high-silica adakite (Moyen, 2009). Lower model HREE for early Earth (and Yanacocha) than for Mount St. Helens may reflect somewhat greater depth of melting (cf. Reimink et al., 2020).

Genetic Constraints on Early Earth Melts

Early Earth model melts were likely influenced by similar petrogenetic conditions as TTG and adakite-like magmas, based on their distinct similarity in REE patterns. The steep negative slope of REE patterns (Fig. 2) and extreme depletion of HREE (Figs. 2 and 3) imply a crystalline residue with strong affinity for the REE. High bulk Kds for HREE, along with the inflection in the middle-heavy REE portion of the patterns, strongly implicate either garnet, amphibole, or both (e.g., Kay, 1978; Moyen, 2009). The median Hadean and Archean patterns with the inflection at Er-Tm (Fig. 2) imply garnet in the residue, as the maximum in the amphibole Kd pattern is at Gd-Dy (Davidson et al., 2013). Such patterns (REE and Kd) and implied mineral residues (garnet +/- amphibole), together with experimental phase equilibria, are attributed to partial melting of eclogitic or amphibolitic mafic sources at moderately high to very high pressure –commonly suggested to be $\geq$1 GPa (e.g., Beard and Lofgren, 1991; Rapp and Watson, 1995), but possibly as low as 0.7 GPa (Newton, 2018). In modern environments, such conditions and source materials imply melting either in a subducting slab or within mafic lower crust influenced by water (e.g., from amphibole dehydration and/or via slab-derived fluid influx) at temperatures lower than those inferred for typical Hadean-Archean geotherms (Hopkins et al., 2008; Harrison, 2009).

IMPLICATIONS

(1) Zircon-saturated melts of Hadean and Archean age were strikingly similar in composition. The oldest Hadean model melts ($\geq$ 4.25 Ga, n = 12) exhibit tantalizing compositional differences that warrant future study.

(2) Hadean-Archean model melts are distinctly different from "primitive" magmas (those of mantle origin, reflecting a high geotherm: Moon, MORB, Iceland, oceanic arcs). They are distinctly similar to modern, adakite-like, arc magmas. As is expected from their dominance in the Archean, TTGs also closely match Archean zircon-modelled melts.

(3) Early Earth model melt REE/ch patterns, with strong HREE depletion and inflections near Er-Tm, suggest generation in the presence of garnet and/or amphibole. This implies petrogenesis in hydrous, high pressure environments that were relatively cool compared to our current understanding of typical Hadean-Archean geotherms.

APPENDIX

1. Zircon data, supporting references, $Kd_{Zrc(Ti)}$, and calculated model melt compositions.
2. Supplemental figures.

ACKNOWLEDGMENTS

This work was supported by NSF grants EAR-0635922 and 1220523.

REFERENCES CITED

Barth, A.P., Tani, K., Meffre, S., Wooden, J.L., Coble, M.A.A., Arculus, R.J.J., Ishizuka, O., and Shukle, J.T.T., 2017, Generation of Silicic Melts in the Early Izu-Bonin Arc Recorded by Detrital Zircons in Proximal Arc Volcaniclastic Rocks From the Philippine Sea: Geochemistry, Geophysics, Geosystems, v. 18, no. 10, p. 3576–3591, doi: 10.1002/2017GC006948.

Barth, A.P., Wooden, J.L., Jacobson, C.E., and Economos, R.C., 2013, Detrital zircon as a proxy for tracking the magmatic arc system: The California arc example: Geology, v. 41, no. 2, p. 223–226.

Beard, J.S., and Lofgren, G.E., 1991, Dehydration Melting and Water-Saturated Melting of Basaltic and Andesitic Greenstones and Amphibolites at 1, 3, and 6. 9 kb: Journal of Petrology, v. 32, no. 2, p. 365–401, doi: 10.1093/petrology/32.2.365.

Bell, E.A., Boehnke, P., and Harrison, T.M., 2016, Recovering the primary geochemistry of Jack Hills zircons through quantitative estimates of chemical alteration: Geochimica et Cosmochimica Acta, v. 191, p. 187–202, doi: 10.1016/j.gca.2016.07.016.

Bell, E.A., Boehnke, P., Hopkins-Wielicki, M.D., and Harrison, T.M., 2015, Distinguishing primary and secondary inclusion assemblages in Jack Hills zircons: Lithos, v. 234–235, p. 15–26, doi: 10.1016/J.LITHOS.2015.07.014.

Bell, E.A., Boehnke, P., and Mark Harrison, T., 2017, Applications of biotite inclusion composition to zircon provenance determination: Earth and Planetary Science Letters, v. 473, p. 237–246, doi: 10.1016/J.EPSL.2017.06.012.

Carley, T.L., Miller, C.F., Wooden, J.L., Padilla, A.J., Schmitt, A.K., Economos, R.C., Bindeman, I.N., and Jordan, B.T., 2014, Iceland is not a magmatic analog for the Hadean: Evidence from the zircon record: Earth and Planetary Science Letters, v. 405, p. 85–97, doi: 10.1016/j.epsl.2014.08.015.

Claiborne, L.L., 2011, Understanding Upper Crustal Silicic Magmatic Systems Using the Temporal, Compositional, and Thermal Record in Zircon: Vanderbilt University, 385 p.

Claiborne, L.L., Miller, C.F., Gualda, G.A., Carley, T.L., Covey, A.K., Wooden, J.L., and Fleming, M.A., 2018, Zircon as Magma Monitor: Robust, Temperature-Dependent Partition Coefficients from Glass and Zircon Surface and Rim Measurements from Natural Systems, *in* Moser, D.E., Corfu, F., Darline, J.R., Reddy, S.M., and Tait, K. eds., Microstructural Geochronology: Planetary Records Down to Atom Scale (Geophysical Monograph 232), John Wiley & Sons, p. 3–34.

Claiborne, L.L., Miller, C.F., Walker, B.A., Wooden, J.L., Mazdab, F.K., and Bea, F., 2006, Tracking magmatic processes through Zr/Hf ratios in rocks and Hf and Ti zoning in zircons: An example from the Spirit Mountain batholith, Nevada: Mineralogical Magazine, v. 70, no. 5, p. 517–543, doi: 10.1180/0026461067050348.

Crow, C.A., McKeegan, K.D., and Moser, D.E., 2017, Coordinated U–Pb geochronology, trace element, Ti-in-zircon thermometry and microstructural analysis of Apollo zircons: Geochimica et Cosmochimica Acta, v. 202, p. 264–284, doi: 10.1016/j.gca.2016.12.019.

Davidson, J., Turner, S., and Plank, T., 2013, Dy/Dy*: Variations Arising from Mantle Sources and Petrogenetic Processes: Journal of Petrology, v. 54, no. 3, p. 525–537, doi: 10.1093/petrology/egs076.

Dilles, J.H., Kent, A.J.R., Wooden, J.L., Tosdal, R.M., Koleszar, A., Lee, R.G., and Farmer, L.P., 2015, Zircon compositional evidence for sulfur-degassing from ore-forming arc magmas: Economic Geology, v. 110, no. 1, p. 241–251, doi: 10.2113/econgeo.110.1.241.

Ferry, J.M., and Watson, E.B., 2007, New thermodynamic models and revised calibrations for the Ti-in-zircon and Zr-in-rutile thermometers: Contributions to Mineralogy and Petrology, v. 154, no. 4, p. 429–437, doi: DOI 10.1007/s00410-007-0201-0.

Gréaux, S., Nishi, M., Tateno, S., Kuwayama, Y., Hirao, N., Kawai, K., Maruyama, S., and Irifune, T., 2018, High-pressure phase relation of KREEP basalts: A clue for finding the lost Hadean crust? Physics of the Earth and Planetary Interiors, v. 274, p. 184–194, doi: 10.1016/J.PEPI.2017.12.004.

Grimes, C.B., John, B.E., Kelermen, P.B., Mazdab, F.K., Wooden, J.L., Cheadle, M.J., Hanghoj, K., and Schwartz, J.J., 2007, Trace element chemistry of zircons from oceanic crust: A method for distinguishing detrital zircon provenance: Geology, v. 35, no. 7, p. 643–646, doi: Doi 10.1130/G23603a.1.

Harrison, T.M., 2020, Hadean Earth: Springer Nature.

Harrison, T.M., 2009, The Hadean crust: evidence from> 4 Ga zircons: Annual Review of Earth and Planetary Sciences, v. 37, p. 479–505.

Hopkins, M., Harrison, T.M., and Manning, C.E., 2008, Low heat flow inferred from >4 Gyr zircons suggests Hadean plate boundary interactions: Nature, v. 456, no. 7221, p. 493–496.

Kay, R.W., 1978, Aleutian magnesian andesites: Melts from subducted Pacific ocean crust: Journal of Volcanology and Geothermal Research, v. 4, no. 1–2, p. 117–132, doi: 10.1016/0377-0273(78)90032-X.

Kemp, A.I.S., Wilde, S.A., Hawkesworth, C.J., Coath, C.D., Nemchin, A., Pidgeon, R.T., Vervoort, J.D., and DuFrane, S.A., 2010, Hadean crustal evolution revisited: New constraints from Pb–Hf isotope systematics of the Jack Hills zircons: Earth and Planetary

Science Letters, v. 296, no. 1, p. 45–56.

Kenny, G.G., Whitehouse, M.J., and Kamber, B.S., 2016, Differentiated impact melt sheets may be a potential source of Hadean detrital zircon: Geology, v. 44, no. 6, p. 435–438, doi: 10.1130/G37898.1.

Kinny, P.D., and Maas, R., 2003, Lu-Hf and Sm-Nd isotope systems in zircon: Reviews in Mineralogy and Geochemistry, v. 53, no. 1, p. 327–341, doi: 10.2113/0530327.

Lowenstern, J.B., Charlier, B.L.A., Clynne, M.A., and Wooden, J.L., 2006, Extreme U–Th disequilibrium in rift-related basalts, rhyolites and granophyric granite and the timescale of rhyolite generation, intrusion and crystallization at Alid volcanic center, Eritrea: Journal of Petrology, v. 47, no. 11, p. 2105–2122, doi: DOI 10.1093/petrology/egl038.

Lowenstern, J.B., Clynne, M.A., and Bullen, T.D., 1997, Comagmatic A-type granophyre and rhyolite from the Alid volcanic center, Eritrea, northeast Africa: Journal of Petrology, v. 38, no. 12, p. 1707–1721.

McDonough, W.F., and Sun, S. -s., 1995, The composition of the Earth: Chemical Geology, v. 120, no. 3–4, p. 223–253, doi: 10.1016/0009-2541(94)00140-4.

Moyen, J.-F., 2009, High Sr/Y and La/Yb ratios: The meaning of the “adakitic signature”: Lithos, v. 112, no. 3–4, p. 556–574, doi: 10.1016/J.LITHOS.2009.04.001.

Moyen, J.F., 2011, The composite Archaean grey gneisses: Petrological significance, and evidence for a non-unique tectonic setting for Archaean crustal growth: Lithos, v. 123, no. 1–4, p. 21–36.

Moyen, J.F., and Martin, H., 2012, Forty years of TTG research: Lithos, v. 148, p. 312–336, doi: 10.1016/j.lithos.2012.06.010.

Newton, R.C., 2018, A Geo-Experimental Diagram for Garnet Amphibolite and Its Bearing on the Origin of Continents: The Journal of Geology, v. 126, no. 5, p. 531–539, doi: 10.1086/698820.

O'Neil, J., Carlson, R.W., Francis, D., and Stevenson, R.K., 2008, Neodymium-142 evidence for Hadean mafic crust: Science, v. 321, no. 5897, p. 1828–1831, doi: 10.1126/science.1161925.

Rapp, R.P., and Watson, E.B., 1995, Dehydration Melting of Metabasalt at 8-32 kbar: Implications for Continental Growth and Crust-Mantle Recycling: Journal of Petrology, v. 36, no. 4, p. 891–931, doi: 10.1093/petrology/36.4.891.

Reimink, J.R., Davies, J.H.F.L., Bauer, A.M., and Chacko, T., 2020, A comparison between zircons from the Acasta Gneiss Complex and the Jack Hills region: Earth and Planetary Science Letters, v. 531, p. 115975, doi: 10.1016/J.EPSL.2019.115975.

Schmitt, A.K., Martín, A., Stockli, D.F., Farley, K.A., and Lovera, O.M., 2013, (U-Th)/He zircon and archaeological ages for a late prehistoric eruption in the Salton Trough (California, USA): Geology, v. 41, no. 1, p. 7–10.

Schmitt, A.K., and Vazquez, J.A., 2006, Alteration and remelting of nascent oceanic crust during continental rupture: evidence from zircon geochemistry of rhyolites and xenoliths from the Salton Trough, California: Earth and Planetary Science Letters, v. 252, no. 3, p. 260–274.

Turner, S., Wilde, S., Wörner, G., Schaefer, B., and Lai, Y.-J., 2020, An andesitic source for Jack Hills zircon supports onset of plate tectonics in the Hadean: Nature Communications, v. 11, no. 1, p. 1241, doi: 10.1038/s41467-020-14857-1.

Valley, J.W., 2003, Oxygen isotopes in zircon: Reviews in Mineralogy and Geochemistry, v. 53, no. 1, p. 343–385, doi: 1529-6466/03/0053-0013$05.00.

FIGURE CAPTIONS:

Figure 1. U/Yb vs Y in zircon-based model melts. (A) Early Earth (Hadean and Archean) vs. modern settings; global compilation of bulk rock tonalite-trondhjemite-granodiorite (TTG) compositions shown for comparison (Moyen, 2011). Symbols represent median model melt compositions; fields show ranges of modeled compositions (extreme outliers excluded). (B) Median Hadean and Archean model melts binned by age. In both A and B, Hadean includes 12 ≥ 4.25 Ga model melts calculated using an assumed Ti concentration of 5 ppm (paired Ti-TE were unavailable). See text and Appendix 1 for data sources.

Figure 2. Median REE patterns of zircon-based model melts. (A) Early Earth vs. modern settings, with bulk rock TTG for comparison (Moyen, 2011). (B) Hadean and Archean model melts binned by age. Model melts ≥ 4.25 Ga (n = 12) were calculated using an assumed Ti concentration of 5 ppm. Note that REE lighter than Nd are excluded, because zircon Kds are unreliable for these extremely incompatible elements (Claiborne et al., 2018). McDonough and Sun (1995) was used for chondrite normalization. See text and Appendix 1 for data sources.

Figure 3. Chondrite normalized REE ratios of early Earth model melts binned by age. Lower and upper edges of the boxes represent the 25^{th} and 75^{th} percentiles. Boxes are bisected by the median. N-values represent population totals. Model melts in ≥ 4.25 Ga bin were calculated using an assumed Ti concentration of 5 ppm. (A) Sm/Lu (MREE/HREE); high ratios are more "adakite-like." (B) Lu/Tm; values >1 indicate slope reversal characteristic of "adakites-like"

magmas and many TTGs. McDonough and Sun (1995) was used for chondrite normalization. See text and Appendix 1 for data sources.

Figure 1

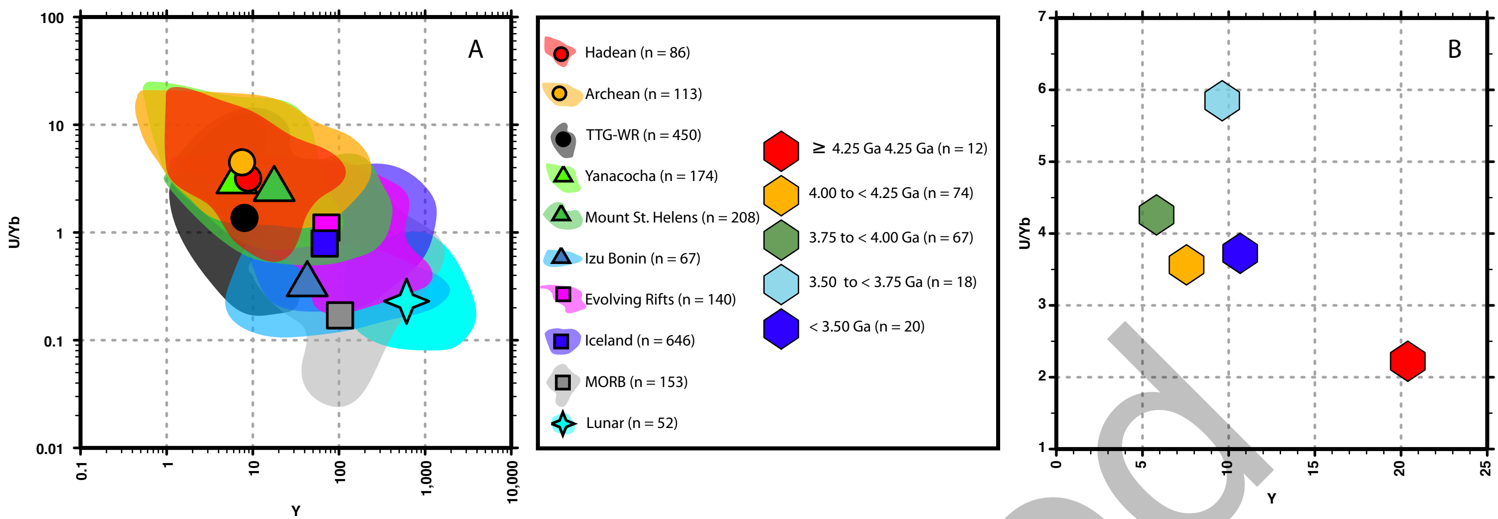
A
B
U/Yb
Y
100
10
1
0.1
0.01
0.1
1
10
100
1,000
10,000
0
5
15
20
25
2
3
4
5
6
7
Hadean (n = 86)
Archean (n = 113)
TTG-WR (n = 450)
Yanacocha (n = 174)
Mount St. Helens (n = 208)
Izu Bonin (n = 67)
Evolving Rifts (n = 140)
Iceland (n = 646)
MORB (n = 153)
Lunar (n = 52)
≥ 4.25 Ga 4.25 Ga (n = 12)
4.00 to < 4.25 Ga (n = 74)
3.75 to < 4.00 Ga (n = 67)
3.50 to < 3.75 Ga (n = 18)
< 3.50 Ga (n = 20)

Figure 2

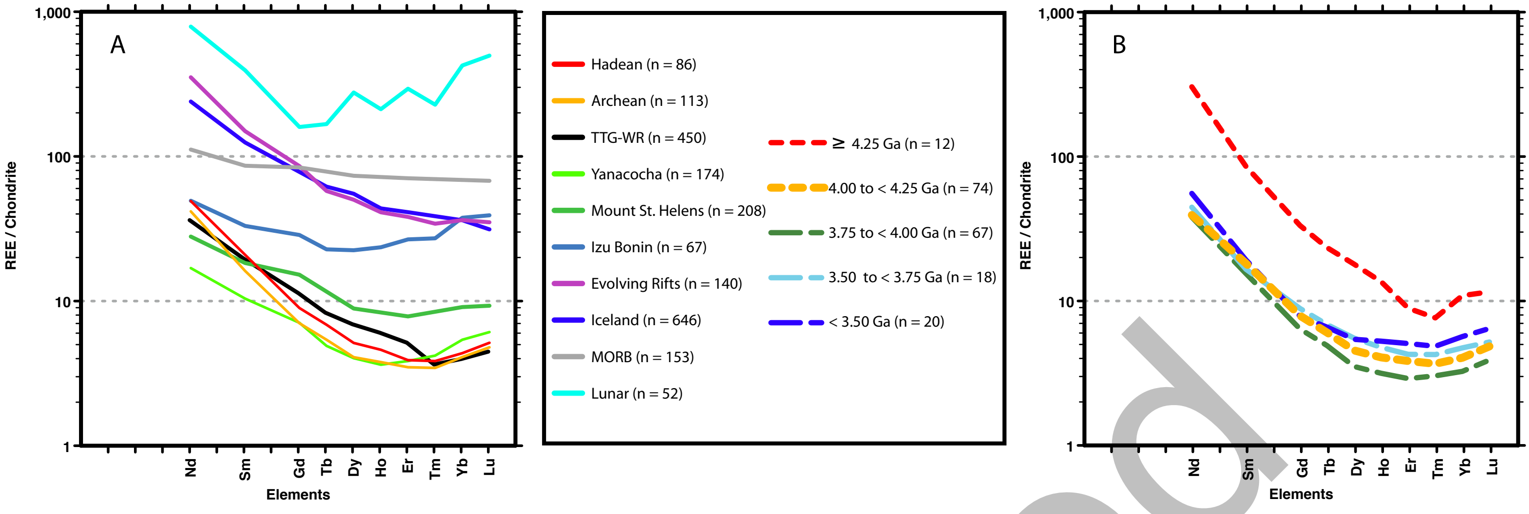

A
1,000
100
10
1
REE / Chondrite
Nd
Sm
Gd
Tb
Dy
Ho
Er
Tm
Yb
Lu
Elements
Hadean (n = 86)
Archean (n = 113)
TTG-WR (n = 450)
Yanacocha (n = 174)
Mount St. Helens (n = 208)
Izu Bonin (n = 67)
Evolving Rifts (n = 140)
Iceland (n = 646)
MORB (n = 153)
Lunar (n = 52)
≥ 4.25 Ga (n = 12)
4.00 to < 4.25 Ga (n = 74)
3.75 to < 4.00 Ga (n = 67)
3.50 to < 3.75 Ga (n = 18)
< 3.50 Ga (n = 20)
B

Figure 3

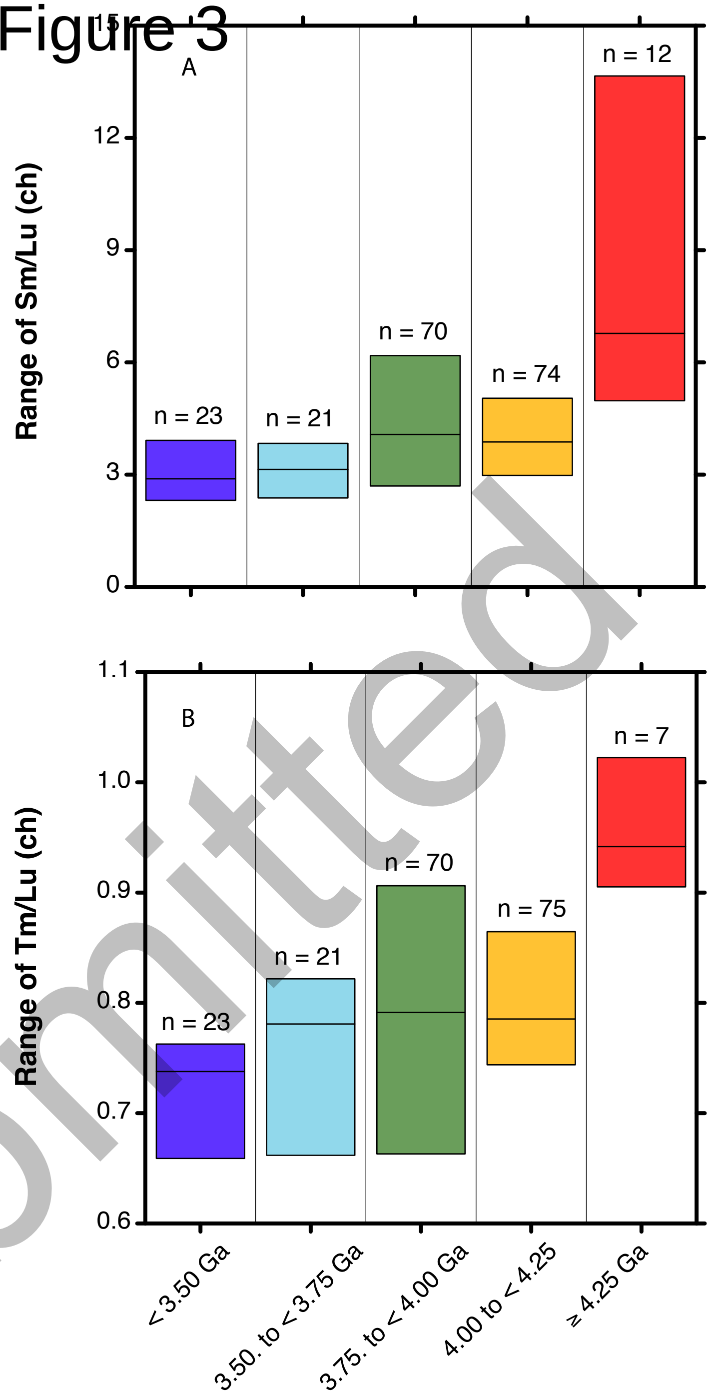

A
n = 23
n = 21
n = 70
n = 74
n = 12
Range of Sm/Lu (ch)
0
3
6
9
12
15
B
n = 23
n = 21
n = 70
n = 75
n = 7
Range of Tm/Lu (ch)
0.6
0.7
0.8
0.9
1.0
1.1
< 3.50 Ga
3.50. to < 3.75 Ga
3.75. to < 4.00 Ga
4.00 to < 4.25
≥ 4.25 Ga